Separation & Purification Reviews
Publication details, including instructions for authors and subscription information:
http://www.informaworld.com/smpp/title~content=t713597294

ISOPYCNIC FOCUSING REVISITED

Josef Janča[a]; Natalia Gospodinova[a]
[a] Université de La Rochelle, La Rochelle, France

Online publication date: 07 October 2000

To cite this Article Janča, Josef and Gospodinova, Natalia(2000) 'ISOPYCNIC FOCUSING REVISITED', Separation & Purification Reviews, 29: 2, 247 — 283
To link to this Article: DOI: 10.1081/SPM-100100011
URL: http://dx.doi.org/10.1081/SPM-100100011

SEPARATION AND PURIFICATION METHODS, 29(2), 247–283 (2000)

ISOPYCNIC FOCUSING REVISITED

Josef Janča* **and Natalia Gospodinova**

Université de La Rochelle, Pôle Sciences et Technologie,
Avenue Marillac, 17042 La Rochelle
Cedex 01, France

ABSTRACT

The isopycnic focusing has for a longtime been considered as a phenomenon occurring exclusively in a fluid which behaves as a continuum with regard to the focused species. It has been shown recently, both theoretically and experimentally, that such an assumption is not necessary and the focusing can appear in a complex fluid composed of bidisperse suspension of the colloidal particles of different but commensurable sizes or in a polydisperse particulate suspension as well. Under such conditions, the question arose about the nature of the driving forces acting on a discrete microscopic scale and generating the macroscopically observed focusing phenomena. In this work, the theoretical analysis is developed to determine the general conditions under which the focusing phenomenon can emerge and to specify the effective driving forces susceptible to contribute to the resulting focusing force. The accompanying experiments were carried out in order to check the particular conclusions following from the theory. On the basis of the general theoretical approach, a new phenomenon, the osmotic pressure gradient focusing (OPGF) is predicted theoretically.

* Corresponding author

INTRODUCTION

The invention of an aerostat floating in the terrestrial atmosphere[1] is based on the macroscopic physical behavior which has been "rediscovered" on the microscopic scale and exploited in generic isopycnic[2] and isoelectric[3,4] focusing processes. Although the macroscopic pattern seems to be very simple, the focusing phenomena show themselves as rather complex processes when descending to the molecular level.

The isopycnic focusing was discovered and applied for the separation purposes by Meselson, Stahl, and Vinograd[2]. The sedimentation (under the effect of the gravitational or inertial centrifugal forces) of the molecules, macromolecules or colloidal particles dissolved or suspended in a simple fluid generates the formation of the concentration (density) gradient. The counteracting diffusion opposes the sedimentation flux until the dynamic equilibrium is reached at which the sedimentation and the diffusion fluxes are balanced. Some of the species dissolved or dispersed (see remark in Appendix) in such a density gradient forming fluid can be focused into the zones at the isopycnic positions where their density is equal to the local density of the complex fluid.

The commonly widespread axiom was that the density gradient forming complex fluid should behave as a continuum with regard to the focused species. It should mean, that the molecules, macromolecules or colloidal particles which form the density gradient should be much smaller compared with the species undergoing the focusing process. On the contrary, it has been predicted theoretically[5] and demonstrated experimentally[6] that such an axiom is not valid and that the focusing phenomenon can appear in bidisperse suspensions of the colloidal particles of the low particle size ratio[7]. Moreover, the focusing phenomenon has experimentally been observed not only in bidisperse suspensions of the colloidal particles of different chemical nature but, just recently, also in a polydisperse suspension of the chemically homogeneous colloidal particles[8]. Subsequent experimental proof of the occurrence of the focusing phenomenon in bidisperse suspension of the colloidal particles of low particle size ratio σ_p was obtained by applying the coupled action of two physical fields of different nature, namely the electric and gravitational[9].

As a result, it became evident that a simple difference between the density ρ_i of the focused species and the local density value $\rho(x,y,z)$ of the density gradient forming fluid combined with the action of the gravitational or centrifugal forces cannot be the unique driving force which generates the observed focusing phenomenon in so called *isopycnic focusing*. Such a simplification is not justified to explain the focusing phenomena in colloidal systems containing the species of the commensurate sizes, some of them creating the density gradient and the other ones being focused. Therefore, various interactions, including the

collisions among all concerned species (molecules, macromolecules or colloidal particles) of the gradient forming fluid as well as the individual species undergoing the focusing transport phenomena, must be taken into account. Consequently, the macroscopic density gradient should not be the true effective property when regarding the focusing processes on the microscopic scale and the resulting phenomenon should be called more accurately *the isoperichoric focusing*. The term isoperichoric (derived from Greek: isos=equal and perichoron=environment) focusing was introduced by Kolin[10] who postulated that the focusing forces are generated by the difference between the responding parameter of the focused sample component and the corresponding local effective property of the dispersing fluid. Therefore, in Kolin's model, a dispersing fluid (an environment) represents, in fact, a continuum and the existence of the nonzero effective property gradient $\partial P/\partial x \neq 0$ which produces the *surface forces* exerting upon the boundary of the focused species combined with the *volume force* acting on the enclosed volume of the focused species is sufficient to generate the isoperichoric focusing phenomena.

In our theoretical approach, a simultaneous action of a unidirectional gradient of the effective property of a dispersing fluid (an anisotropy) and of an external or intrinsically generated unidirectional field force is necessary for the focusing phenomenon to occur. The coupled action of the intrinsic gradient and of the external field originates the driving force whose intensity and sign changes with the spatial position within the system and leads to the formation of the zones of the focused species. Each dispersed species can form an individual focused zone. The existence of the driving force whose intensity varies with the direction of the x-axis (which is parallel to the direction of the focusing) and vanish at the position where the particular zone is focused is therefore a fundamental condition for the focusing phenomena to appear. However, we will develop our model further to show that a simple condition $\partial P/\partial x \neq 0$ should not be sufficient in all instances for the isoperichoric focusing phenomena to emerge.

The isopycnic focusing centrifugation is considered as a method of choice for the characterization of the colloidal and macromolecular systems[11]. Its recent theory and practical experimental use are based on a macroscopic phenomenological model. The aim of this work is to study theoretically the macroscopic transports and the microscopic interactions generating and accompanying the focusing phenomena in order to determine the conditions under which the isoperichoric focusing can occur. The experimental part is aimed basically to verify the conclusions of the theoretical predictions and estimations. Although the primary objective is to study in detail the isoperichoric focusing due to the gravitational or centrifugal forces, the possible use of the coupling of other field forces and gradients is considered and discussed.

THEORY

Dynamic Transport Model

This theoretical model represents a macroscopic approach which does not require, in a first approximation, to look at the microscopic interactions to calculate the effect of various parameters (including the size ratio σ_p of the focused to the density gradient forming discrete species) on the focusing phenomena. The density gradient forming medium is a two phase fluid consisting of uniform size colloidal particles (modifier) dispersed in a homogeneous liquid and enclosed between two parallel plates which are large enough to make the effect of the side walls negligible. The other advantage of such a model is that it should not, also in a first approximation, take into account the effect of the concentration (volume fraction) of the modifier on the transport coefficients. The local volume fraction of the modifier determines therefore only the magnitude of the effective environmental (perichoric) property of the complex fluid, the density for instance. The initial volume fraction of the modifier is uniform over the whole system and equal to the average volume fraction:

$$\phi_m(x,y,z,t=0) = \phi_{m,ave} \tag{1}$$

The fluid is macroscopically isotropic at the time $t=0$, the only fluctuations of the volume fraction are due to the Brownian movement. For the time $t>0$, the dispersed modifier particles undergo the transport phenomena due to the imposed effective field forces and the counteracting dispersive migration. The unidirectional concentration (volume fraction) gradient $dc_m/dx = \rho_m d\phi_m/dx$ of the modifier is formed and the fluid exhibits an anisotropy of the effective property in the direction of the effective field induced flux. The total macroscopic mass flux of the modifier moving in the direction of the x-axis (which is parallel with the direction of the effective field forces, the origin $x=0$ is at the accumulation wall and the positive direction toward the depletion wall) can be written as the number n_m of the particles of a uniform volume v_m and of the density ρ_m which pass across a unit surface area s (perpendicular to the field induced flux) in a unit time t:

$$J_{x,m} = \rho_m \frac{v_m \partial n_m}{s \partial t} \tag{2a}$$

and the macroscopic fluxes $J_{y,m}$ and $J_{z,m}$ are at any time $t \geq 0$:

$$J_{y,m} = 0 \qquad \text{and} \qquad J_{z,m} = 0 \tag{2b}$$

The term macroscopic flux is used here to describe the bulk mass transport of the modifier due to the imposed field forces. The thermal molecular motion or Brownian migration on a microscopic scale as well as secondary convective fluxes (microturbulence or the suspending liquid flux compensating the displacement of the

modifier) due to the field induced selective transport are not taken into account in this macroscopic dynamic transport model regardless the fact that $j_{x,y,zm} \neq 0$ at any $t \geq 0$. The lower-case j is used to distinguish the microscopic scale flux from the macroscopic one J.

The flux $J_{x,m}$ can be decomposed into two contributions, the effective field induced convection $J_{x,m,c}$, and the dispersive migration $J_{x,m,d}$, as mentioned above:

$$J_{x,m,c} = -U_m(c_m)c_m \tag{3}$$

$$J_{x,m,d} = -D_m(c_m)\frac{dc_m}{dx} \tag{4}$$

$$J_{x,m} = J_{x,m,c} + J_{x,m,d} = -U_m(c_m)c_m - D_m(c_m)\frac{dc_m}{dx} \tag{5}$$

where $U_m(c_m)$ and $D_m(c_m)$ are the concentration (volume fraction) dependent transport coefficients (sedimentation velocity and diffusion coefficient, respectively) which must be expressed in units coherent with the concentration. It holds at the infinite time:

$$\lim_{t \to +\infty} J_{x,m} = 0 \tag{6}$$

and such a dynamic quasi-stationary state (equilibrium) is then described by:

$$-\frac{U_m(c_m)}{D_m(c_m)}\,dx = \frac{1}{c_m}\,dc_m \tag{7}$$

The position dependent driving force, $F_i(x)$, generates the macroscopic transport of the focused species i with the position dependent velocity, $U_i(x)$. An effective property gradient of the complex fluid (the density gradient in the case of isopycnic focusing) is either created coincidentally with the focusing processes or preformed beforehand. The dispersive processes act against the formation of the density gradient as well as against the focusing transport until the steady-state is reached. The density gradient forming and the focusing fluxes can be described as two independent processes. This is justified by the fact that the evolution of the focusing processes is faster than a simple settling of the transported species[12]. The total flux in the direction of the x-axis, J_x, is the sum of the flux of the density modifier, $J_{x,m}$, and of the flux of the focused species, $J_{x,f}$:

$$J_x = J_{x,m} + J_{x,f} \tag{8}$$

As mentioned above, the total macroscopic fluxes in the direction of the y and z axes are zero which allows to simplify the notation by removing the subscript χ for all corresponding variables. The velocity of the sedimenting species, U_m, is a negative magnitude with regard to the above defined coordinate system while the focusing force $F_i(x)$ and, consequently, the velocity of the focused species, $U_i(x)$, in the direction of the x-axis must be position dependent, converg-

ing, changing the sign at $x_{i,max}$, and vanish at this focusing point:

$$\begin{array}{llllll} F_i(x) = f(x) & & U_i(x) = f(x) & \text{within } 0 < x < h & & \\ F_i(x) = 0 & \text{and} & U_i(x) = 0 & \text{for} & x = x_{i,max}, & 0 < x_{i,max} < h \\ F_i(x) > 0 & \text{and} & U_i(x) > 0 & \text{for} & x < x_{i,max}, & \\ F_i(x) < 0 & \text{and} & U_i(x) < 0 & \text{for} & x > x_{i,max}, & \end{array} \tag{9}$$

where h is the distance between the accumulation and depletion walls which corresponds to the height of the column of fluid in the sedimentation cell. The $x_{i,max}$ corresponds to the position at which the concentration distribution of the i-th focused species reaches its maximal value. When neglecting, as a first approximation, the dependence of the transport coefficients on the concentration, the J_m and J_f fluxes can be written as:

$$J_m = -D_m \frac{\partial c_m}{\partial x} - U_m c_m \tag{10}$$

$$J_i = -D_i \frac{\partial c_i}{\partial x} + U_i(x) c_i \tag{11}$$

where D_m, D_i, are the diffusion coefficients and c_m, c_i, are the concentrations of the density modifier and of the i-th focused species, respectively, expressed in coherent units. The total flux of all focused species is:

$$J_f = \sum_{i=1}^{n} J_i \tag{12}$$

It holds at the dynamic equilibrium on a macroscopic scale:

$$J = \frac{\partial c}{\partial t} = 0 \tag{13}$$

For J_m=0, the solution of the eqn.(10) is:

$$c_m(x) = c_m(0) \exp(-xU_m/D_m) \qquad \text{with} \qquad c_m(0) = c(x_{m,max}) \tag{14}$$

The exponential concentration distribution, eqn.(14), was already derived by Einstein[13] and verified experimentally by Perrin[14]. It holds for the average concentration, $c_{m,ave}$:

$$c_{m,ave} = \frac{\int_0^h c_m(x)dx}{\int_0^h dx} = c_m(0) \frac{D_m}{hU_m} (1 - \exp(hU_m/D_m)) \tag{15}$$

The substitution into the eqn.14 leads to:

$$c_m(x) = \frac{c_{m,ave} hU_m}{D_m (1 - \exp(-hU_m/D_m))} \exp(-xU_m/D_m) \tag{16}$$

The focusing driving force $F_i(x)$ can be written as:

$$F_i(x) = U_i(x) f_i \tag{17}$$

where f_i is the friction coefficient:

$$f_i = \frac{kT}{D_i} \tag{18}$$

k is Boltzmann constant and T is the absolute temperature. Then it holds:

$$\frac{\partial c_i}{\partial x} = -\frac{F_i(x) c_i}{kT} = -\frac{U_i(x) c_i}{D_i} \tag{19}$$

The eqn.(16) can be rewritten in terms of the densities instead of concentrations:

$$\rho(x) = \rho_l + \frac{\phi_{m,ave} \Delta\rho_m h U_m}{D_m(1 - \exp(-hU_m/D_m))} \exp(-xU_m/D_m) \tag{20}$$

where $\Delta\rho_m = \rho_m - \rho_l$, ρ_l is the density of the dispersing liquid, and $\phi_{m,ave}$ is the average volume fraction of the density modifier particles. The focusing force acting on a single focused species is:

$$F_i(x) = (\rho(x) - \rho_i) v_i g \tag{21}$$

where v_i is the volume of one focused macromolecule or particle and g is the gravitational or centrifugal acceleration. The solution of the eqn.(19) is[5,7]:

$$c_i(x) = c_i(x_{i,max}) \exp\left\{-\left[\frac{v_i g \phi_{m,ave} \Delta\rho_m h}{kT(1 - \exp(-hU_m/D_m))}\right] \times \left[\exp(-xU_m/D_m) - \exp(-x_{i,max}U_m/D_m)\left(1 + \frac{U_m(x_{i,max} - x)}{D_m}\right)\right]\right\} \tag{22}$$

The eqn.(22) describes, in principle, the probability that a single focused particle of the volume v_i (whose density corresponds to the density of the liquid at the position $x_{i,max}$ within the density gradient) appears at a given position x. Or, in a practical sense, it describes the steady-state concentration distribution of the focused species i superposed over the established density gradient[5,7]. An accurate application of the eqn.(22) is conditioned by the physical limits which cannot be overcome. The high value of the centrifugal acceleration and/or the extremely low (theoretically calculated) diffusion coefficient of the large size density gradient forming species can result in excessively high values of the ratio U_m/D_m. In such a case, the theoretically calculated $c_m(0)$ can reach physically impossible high values. From the experimental point of view, such a situation can result in the formation of a compact cake at the bottom of the sedimentation cell. The second complication is that the transport coefficients U_m and D_m can be dependent on the

concentration as mentioned above due to the increased importance of all kind of interactions between the sedimenting species at high concentrations. This problem was already studied by Batchelor[15], Clercx and Schram[16], and the authors cited therein. We have shown recently[17,18] that the electrostatic repulsions are largely dominating over the hydrodynamic interactions in the investigated systems, representing the most typical cases.

As concerns the focused species, we consider them, in a first approximation, as the isolated spheres (surrounded only by the modifier species) not interacting with each other and not interacting specifically with the modifier species. This assumption will be reconsidered later when developing the kinetic model. The dynamic transport model does not require to consider the specific interactions of the focused species.

The dynamic transport model predicts the focusing with no a priori imposed size ratio σ_p of the focused to the density gradient forming species. A detailed computer simulation of the effect of operational variables on the width and shape of the focused zone was performed and described in our previous paper[7]. The most important conclusions of this simulation are as follows:

1. The focused zones are larger for lower accelerations mainly due to the weaker density gradient.
2. The width of the focused zone increases with the decreasing steepness of the density gradient.
3. When the initial suspension of the modifier species is less concentrated, the established density gradient is weaker and the focused zones are larger again.
4. The density gradient is weaker for lower h values and, consequently, the zones are relatively larger when the zone width is expressed in terms of the dimensionless x/h-coordinate.
5. The simulation of the focusing phenomenon in bidisperse suspension of the colloidal particles of the low size ratio σ_p indicated that the focused zones became progressively larger when the size ratio decreased but the focusing phenomenon completely disappeared only when this ratio approached to 1.

All these predictions result directly from the eqn.(22). They were partly verified by the focusing of the polyaniline nanosize particles in a density gradient formed by colloidal silica particles suspended in water, by applying the centrifugal field forces[6] or a combination of the electric and natural gravitational fields[9]. The size ratio σ_p of the polyaniline to silica particles was low. The results of a more detailed investigation of the validity of the previous theoretical predictions and the extension of the computer simulation are described in this paper.

Kinetic Model

The initial conditions in this microscopic (or mesoscopic, i.e., on particle size scale) approach are the same as in the case of the dynamic transport model. The system is a two component complex fluid consisting of uniform size and mass colloidal particles dispersed in a homogeneous liquid enclosed between two parallel plates. The equilibrium concentration distribution of the density modifier is established due to the action of the external (e.g., centrifugal) field forces. The microscopic fluctuations of the local volume fraction are due to the dynamic character of the equilibrium which is permanently perturbed by the Brownian movement resulting from the thermal molecular motion. The focused species behave as individual spheres surrounded by the density modifier particles and by the molecules of the suspending liquid.

The modifier particles exert frequent collisions with the focused particles providing that the volume fraction of the modifier particles is high enough with respect to the focused ones. The *j*-th modifier particle entering into the collision with a focused particle during a period of time between t and $t+\tau$ acts on the focused particle with a force $F_{i,j}$. The average force acting on the focused particle during the period τ is given by:

$$\langle F_{i,j} \rangle = \frac{1}{\tau} \int_t^{t+\tau} F_{i,j} dt \tag{23}$$

On the other hand, the focused particle reacts towards the *j*-th interacting modifier particle by an opposite force $F_{m,j}$ of the same magnitude:

$$F_{m,j} = m_m \frac{du_m}{dt} = -F_{i,j} \tag{24}$$

where m_m is the mass and u_m is the velocity of the modifier particle in the moment of the collision. By substituting into eqn. (23) we obtain:

$$\langle F_{i,j} \rangle = -\frac{1}{\tau} \int_t^{t+\tau} m_m \frac{du_m}{dt} dt \tag{25}$$

and:

$$\langle F_{i,j} \rangle = \frac{1}{\tau} (m_m u_{m,imp} - m_m u_{m,reb}) \tag{26}$$

where $u_{m,imp}$ and $u_{m,reb}$ are the velocities of the modifier particle before the impact and after the rebound, respectively. The sum of the collisions of all interacting modifier particles during the time τ gives the overall force:

$$\sum_{j=1}^{n} \langle F_{i,j} \rangle = \frac{1}{\tau} \left(\sum_{j=1}^{n} m_m u_{m,imp} - \sum_{j=1}^{n} m_m u_{m,reb} \right) \tag{27}$$

It holds for a large number of the modifier particles at the dynamic equilibrium that the total momentum is zero and, therefore:

$$\sum_{j=1}^{n} m_m u_{m,imp} = -\sum_{j=1}^{n} m_m u_{m,reb} \tag{28}$$

The eqn. (27) can be rewritten to obtain:

$$F_i = \sum_{j=1}^{n} \langle F_{i,j} \rangle = \frac{2}{\tau} \sum_{j=1}^{n} m_m u_m \tag{29}$$

where F_i is the resulting force acting on the focused particle at the dynamic equilibrium.

By defining the pressure Π_i as the force per unit area σ of the surface of the focused spherical particle (see Fig.1), it holds:

$$\Pi_i = \frac{2}{\tau\sigma} \sum_{j=1}^{n} m_m u_m \tag{30}$$

During the time τ, the modifier particles travel, in average, the distance $\langle u_{m,j} \rangle \tau$. It means, that the fraction $X n_m \langle u_{m,j} \rangle \tau$ of all modifier particles whose number in unit volume element is n_m generates the pressure Π_i:

$$\Pi_i = 2X n_m m_m \langle u_{m,j} \rangle^2 \tag{31}$$

where the X represents a fraction of the *x*-axis components of all trajectories of the moving modifier particles, σ is already equal to one. The eqn.(31) is an analogy of the Clausius' kinetic theory equation for the gas pressure for which $X = 1/6$ and the Π_i has the physical meaning of the partial osmotic pressure of the modifier particles. The right hand side of the eqn.(31) represents the kinetic energy of the translational movement of the concerned particles (molecules). It can be rewritten as:

$$\Pi_i = n_m kT \tag{32}$$

The number of the modifier particles n_m in unit volume element varies with the position χdue to the action of the primary (gravitational, centrifugal, or other) external field. The equilibrium distribution $n_m(x)$ results in a partial osmotic pressure gradient:

$$\frac{d\Pi_l}{dx} = kT \frac{\partial n_m(x)}{\partial x} \tag{33}$$

The eqn.(33) implies that if, e.g., the $n_m(x)$ is a linear function of *x*, such as:

$$n_m(x) = C_1 + C_2 x \tag{34}$$

C_1 and C_2 being the constants, the gradient of the partial osmotic pressure is:

$$\frac{d\Pi_i}{dx} = kTC_2 \tag{35}$$

Such a gradient produces constant unidirectional force which has to be compensated to satisfy the above mentioned dynamic equilibrium:

$$F_i = kTn_m(x) - F_e \tag{36}$$

Here, F_e is a compensating force generated by the primary or secondary external field. Whenever $F_e=0$ and no other force is effective, the focused particles are displaced in the direction of the x-axis at the extreme limit of the system without exhibiting a focusing phenomenon. On the other hand, the counteracting forces F_i and F_e represent potential focusing force but, as demonstrated above, the focusing can appear only under conditions imposed by the eqns.(9). It means that constant gradient of the partial osmotic pressure, eqns.(34) and (35) cannot, in principle, generate the focusing phenomenon in the absence of other x-axis dependent driving force.

Hyphenated Dynamic-Kinetic Model

We have already shown[5,19] that although the constancy of the density (or osmotic pressure) gradient within the range of the focused zone in isopycnic focusing is often assumed, it is not physically substantiated and the Gaussian distribution resulting from the calculations does not approximate well the concentration distribution of the focused species compared with the accurate distribution function given by the eqn.(22). Moreover, the eqns.(9) and (33) to (36) demonstrate clearly that the appearance of the focusing phenomenon under the conditions of constant gradient of the partial osmotic pressure alone is impossible. On the other hand, the use of the physically substantiated eqn.(16) to describe the concentration distribution of the modifier particles in eqn.(36) leads to the relationship:

$$F_i(x) = kTn_m(x) - F_e \tag{37}$$

in which the driving force $F_I(x)$ varies with the x-coordinate because the substitution for $n_m(x)$ from the eqn.(16) into the eqn.(33), after the corresponding transformation of the variables $c_m(x)$ into $n_m(x)$, does not result into a constant value of the partial osmotic pressure gradient. The conditions imposed by a series of eqns.(9) for the focusing phenomena to appear are thus respected. For example, a spherical particle of the radius r_i situated at the position x_i (see Fig.1) exerts the action of the internal force:

$$F_{i,s}(x) = 2\pi r_i \left[\int_{x_i - r_i}^{x_i} (\Pi_i(x))dx - \int_{x_i}^{x_i + r_i} (\Pi_i(x))dx \right] \tag{38}$$

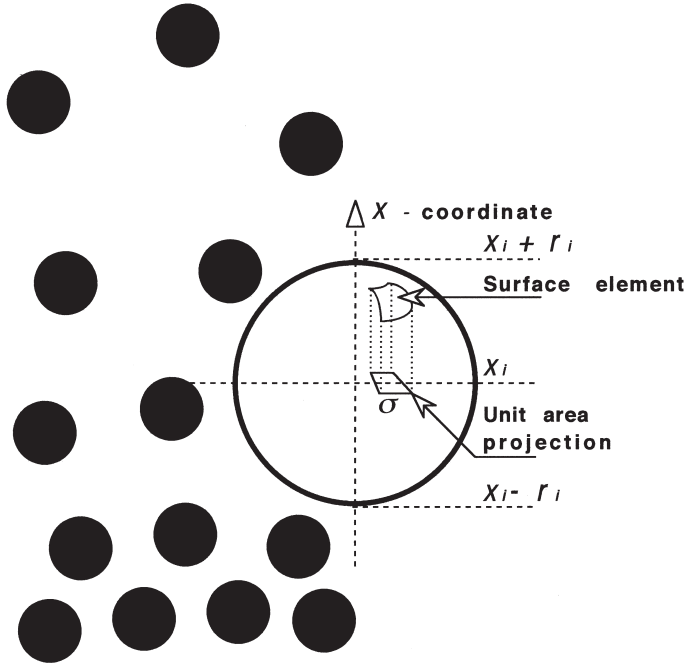

Figure 1. Schematic representation of the interactions of the colloidal density modifier particles forming the concentration (density) gradient in the direction of the *x*-coordinate with the focused particle of a larger but commesurable size.

which is the difference between the integral osmotic pressures on the surface projections of the low and high (with respect to the horizontal plane at $x_{i,max}$) hemispheres. The substitution of the concentration distribution of the modifier particles for the osmotic pressure distribution in eqn.(38) gives:

$$F_{i,s}(x) = 2\pi r_i kT \left[\int_{x_i - r_i}^{x_i} (n_m(x))dx - \int_{x_i}^{x_i + r_i} (n_m(x))dx \right] \tag{39}$$

The resulting focusing force $\overset{\perp}{\boldsymbol{F}}_i$ can be composed of three main contributing forces, namely the internal "lift" force $F_i(x)$, the volume force F_o generated by the primary external field due to the bulk perichoric property of the suspending liquid (such as the Archimedes force), and the force F_e due to the secondary external field, according to:

$$\overset{\perp}{\boldsymbol{F}}_i(x) = F_i(x) - F_e + F_o \tag{40}$$

As a result, a simple action of the secondary field force is not sufficient to produce the focusing effect. At least one of the above specified contributing forces

must be position dependent. In principle, each of the three forces can be a function of the position in the direction of the *x*-axis.

As concerns the particular case of the "isopycnic" focusing, the force F_o, which is due to either gravitational or centrifugal field, can be considered as independent on the position in the direction of the *x*-axis due to the low compressibility of simple liquids. Nevertheless, whenever the strength of the primary (centrifugal) field is high, the variation of the $F_o(x)$ as a function of the *x*-coordinate cannot be neglected

The force F_e can also vary with the *x*-coordinate although its constant magnitude throughout the whole system is the most probable and frequent case, especially in "isopycnic" focusing.

On the other hand, the eqn.(40) shows that even if the volume force F_o is zero, the focusing phenomenon can appear as well, e.g., when both modifier and focused particles migrate due to the action of the external electric field under the microgravity or isodensity conditions. The focusing in such a case will be due to, exclusively, the existence of the osmotic pressure gradient coupled with the constant strength field. While the osmotic pressure gradient appears only as a contributing factor on a microscopic scale in macroscopic "isopycnic" focusing, it becomes the principal driving force under the isodensity conditions. Correspondingly, the focusing phenomenon can rigorously be called the osmotic pressure gradient focusing (OPGF) or, by sacrificing the rigor (which is already the case of the term "isopycnic" focusing), simply the *iso-osmotic focusing*.

Although the kinetic model developed here seems not to be very complicated, the mesoscopic and microscopic collision mechanisms concerning the modifier and focused species can be quite complex. In many cases, the long range interactions (e.g., the electrostatic repulsions) and, consequently, very "elastic" collisions among the modifier and focused species will be effective instead of "true and hard body-body" collisions. Moreover, the electrostatic interactions can lead to the formation of the organized structures of the type of liquid crystals with the consequence such as the "structuring" of the thermodynamic and kinetic equilibrium conditions.

Regardless these potential complications, the presented kinetic model allows a deep insight into the microscopic scale interactions among the active components participating on the "isopycnic" focusing processes. It complements our former dynamic model theory by giving the accurate physical meaning to the behaviors discovered previously by the computer modelling and confirmed partially by the experiments, mainly as concerns the effect of the modifier and focused particle sizes ratio σ_p on the width of the focused zone.

EXPERIMENTAL

The experiments were carried out to check the theoretical approach. Some of the experiments were already performed and their results published, neverthe-

less, the material used and the methodology applied in this work were improved further to achieve the highest accuracy and precision possible recently.

Materials

Commercial product Percoll (Pharmacia Fine Chemicals AB, Sweden), consisting of colloidal silica particles coated with poly(N-vinyl pyrrolidone) (PVP) and suspended in water was used as the density gradient forming liquid. The original product having the density of 1.128 g/ml was diluted with deionized water or with NaCl solutions to obtain the suitable density gradient forming liquids with the known concentrations of NaCl.

Each density gradient forming liquid was treated in an ultrasonic bath to destroy the casual aggregates of the silica particles. The size distributions of the particles in suspension were controlled by the quasi-elastic laser light scattering measurements by using model Zetamaster (Malvern Instruments, Ltd., Malvern, Worcestershire, U. K.) apparatus. No aggregate formation was detected in ultrasonically treated Percoll based liquids.

Ultra-narrow particle size distribution (PSD) composite particles of polyaniline-polyvinylalcohol (PANI-PVA) and poly(*m*-toluidine)-polyvinylalcohol (PMTD-PVA) of various average sizes were prepared especially for this purpose. Their careful synthesis and detailed characterization were subject of the separate studies whose results were published recently[20,21]. The PSDs of all samples were measured by the quasi-elastic laser light scattering mentioned above. As concerns these measurements, the special precautions were adopted and a complete characterization of the samples was performed by using other methods such as the viscometry, scanning electron microscopy (SEM), and centrifugation. All these results are published recently[21]. Here we present in Fig.2 just the PSDs of the silica particles, PANI-PVA and PMTD-PVA composite particles, and, for the comparison, of the commercially available uniform polystyrene microspheres. The Fig.3 shows the SEM picture of the PANI-PVA composite particles demonstrating their spherical form.

Density marker beads, Pharmacia Fine Chemicals AB (Sweden), which are the colored cross-linked dextran particles with defined buoyant densities were used to determine experimentally the shape of the established quasi-equilibrium density gradients. The densities of the marker beads vary slightly with the ionic strength[22]. The manufacturer's buoyant density values of the marker beads can be used only for Percoll solutions diluted with 0.15 M NaCl water solutions. As our solutions of Percoll of given densities were prepared by diluting with deionized water or with NaCl solutions of different concentration, the true buoyant densities were determined experimentally. The detailed experimental data as well as the description of the technique of determination of the buoyant densities of density marker beads are given in our recent paper[17].

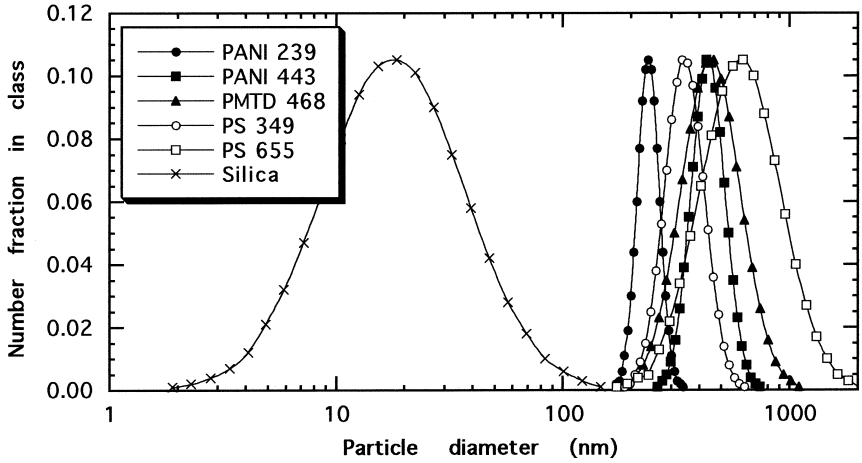

Figure 2. Particle size distributions of some of the applied colloidal particles of the polyaniline, poly(*m*-toluidine), polystyrene, and silica. The average particle diameter of each represented sample is given in nm.

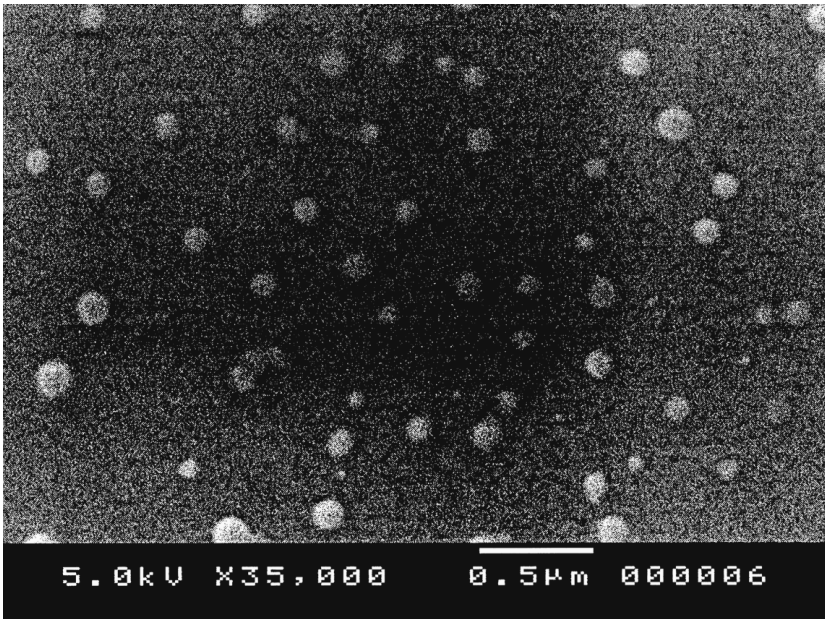

Figure 3. Scanning electron microscopy of the PANI-PVA sample of the average particle size of 443 nm, measured by the quasi-elastic light scattering.

Apparatuses for Thin Layer Isoperichoric Focusing

The centrifugation focusing experiments were performed in a closed glass cell of rectangular cross-section at constant $g = 1.962 \times 10^5$ cm sec^{-2} (200 G). All experiments were carried out at 25°C. The macrophotographs of the steady-state focused zones of the colored PANI-PVP particles in the transparent and colorless silica-PVP suspension were taken by using a standard camera and a black and white film. The image was computer processed by using a suitable software to obtain the experimental concentration distribution of the focused species. More experimental details can be found in our preliminary communication[6].

Thin layer isoperichoric focusing (TLIF) in electrical field was carried out by using a simple apparatus described in our previous papers[9,23]. The closed rectangular cross-section 10x10 mm in size TLIF cells made of polystyrene were used. The distance of 10 mm between the electrodes determined the height of the liquid in the cell. The regulated electric power was supplied from a battery equipped with a potentiometer and a voltmeter. The pictures of the focused zones were taken as in the centrifugation experiments.

Image Processing

The PANI-PVA and PMTD-PVA are green or blue particles whose color varies with the pH while the silica-PVP suspension is transparent light-yellow liquid. The amount of the colored particles in the initial mixture with Percoll for the focusing experiments was adjusted to obtain the optimal distribution of the color intensity within the focused zone and, consequently, the highest possible precision of the numerical readouts. The concentrations of the particles lay within the range of the linear relationship between the concentration and absorption. This relationship was determined by a calibration with a series of images of the homogeneous particle suspensions at different concentrations. The experimental concentration distributions within the focused zones were determined by using the scanned macrophotographs. The digitized images were transformed into the grayscale readouts by a suitable computer processing. The maximal values of the grayscale readouts corresponded to the volume fraction $\phi = 1.75 \times 10^{-5}$ of the colored particles.

A standard camera and a black and white film were chosen to take the original pictures because of their higher optical resolution compared with the numerical cameras. A yellow filter with a sharp cut-off at 500 nm was used with respect to the absorption spectra of the colored particles and silica-PVP modifier particles. The ratio of the PANI-PVA or PMTD-PVA to the silica-PVP absorbances for the above mentioned volume fraction is 20 or higher at 500 nm and rapidly increases with the wavelength. The use of the reflected polychromatic flash allowed to take

the pictures under suitable conditions. The experimental details were published previously[7].

RESULTS AND DISCUSSION

Various effective fields, gradients, and their combinations can, in principle, be applied to generate the focusing effect[24]. The isopycnic focusing is usually due to the action of the gravitational or centrifugal forces in a density gradient formed by the same, primary field. Either the primary field forces establishing the isoperichoric gradient in a complex fluid, or the secondary field forces of different nature coupled with the established gradient can lead to the focusing effect. In this work, the inertial centrifugal or the electrical field forces were applied to generate the density gradient in suspended silica-PVP particles and the focusing of PANI-PVA or PMTD-PVA particles.

Our parallel investigations[17,18] dealt with the transport phenomena underlying the isoperichoric focusing, starting from the kinetics of the transient state to the dynamic equilibrium. The results of these studies allowed to define the operational conditions under which the experiments presented in this work had to be carried out to obtain the accurate results. The equilibrium density gradient established under various operational conditions as well as the kinetic data describing the transient period between the initial uniform distribution of the gradient forming colloidal particles and the equilibrium state allowed to determine the effective ratio of the sedimentation velocity to the diffusion coefficient of the modifier particles by applying the methodology described in previous papers[17,18]. This ratio is necessary for the calculation of the concentration distribution of the focused particles.

Computer Simulation

The dynamic transport model resulting in eqn.(22) was used previously[7] to calculate $c_i(x)$ functions for various input parameters. The intention was to demonstrate their effect on the resulting shape of the concentration distribution of the focused species. Although it is not useful to reproduce all previous calculations here, the results of the computer modeling of the effect of the size ratio σ_p of the modifier to the focused particles is shown in Fig.4 in order to compare further the results of the experiments with those following from the theory. The constant input data for the calculations were: the diameter of the density gradient modifier particles d_m=30 nm, the density difference $\Delta\rho_m$=1 g cm^{-3}, the centrifugal acceleration g=9.81x10^4 cm sec^{-2} (100 G), the average volume fraction ϕ_{mave}=0.1, the height of the column of liquid, h=1 mm, and the ratio σ_p of par-

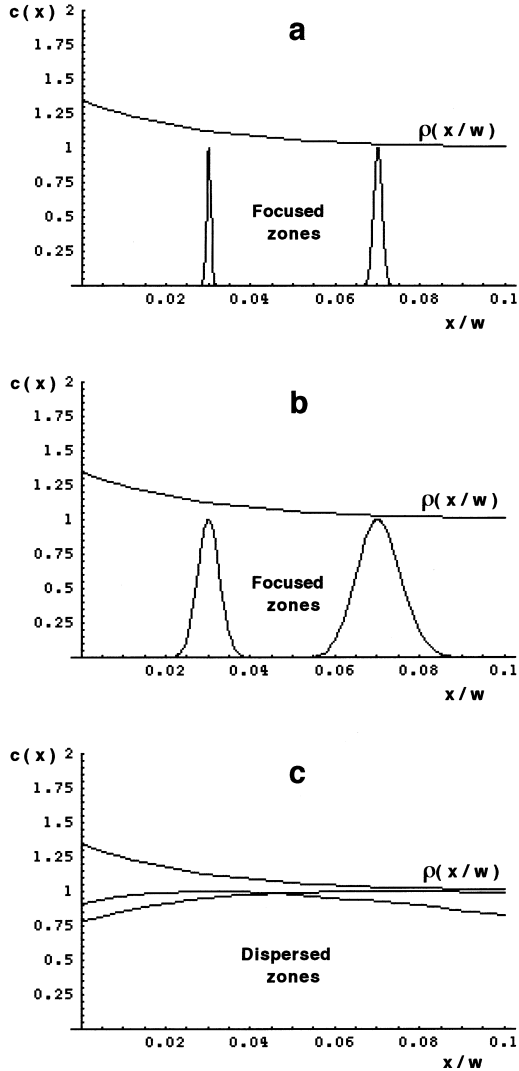

Figure 4. Concentration distributions of the focused particles calculated theoretically from the eqn.(22) for two different positions $x_{i,max}$ in the established density gradient ρ (x/w) and for different focused to modifier particle size ratios σ_p. (**a**) σ_p=10; (**b**) σ_p=3; (**c**) σ_p=1.

ticle diameters of the modifier to the focused species, 30, 10, and 1. The acceleration g is expressed explicitly in the first exponential term of the eqn.(22) but implicitly is comprised in the U_m/D_m ratio. The densities of the two different focused particles are determined by the dimensionless positions $x_{imax}/h=0.3$ and 0.7 of the maximal concentrations $c_i(x_{imax})$. These input data represent typical experiments and are close to the real conditions used in the following experiments.

The upper curves in Fig.4 a,b,c demonstrate the shape of the density gradient $\rho\,(x/w)$ versus the dimensionless coordinate x/w, the lower curves are the normalized concentration distributions, $c_i(x)/c_i(x_{imax})$, of two different densities but uniform size focused particles. The focused zones are very narrow for the particle size ratio $\sigma_p=30$ and become larger as this ratio decreases. The focusing phenomenon practically disappears and the zones are largely dispersed for the size ratio 1. Further decrease of the size ratio of the focused to the modifier particles makes the focusing completely vanish, independently of the imposed size ratio value below 1. A weak tendency to display the focusing which can be seen in Fig.4 c for the size ratio $\sigma_p=1$ is probably due to the inherent precision of the numerical calculus.

Concentration Distribution of the Modifier Particles

The concentration distribution of the modifier particles (the density gradient) is one of the factors determining the width of the focused zones. As the silica-PVP modifier particles are charged, the steepness of the density gradient does not depend on the strenght of the centrifugal field only but also on the concentration of the ions in solution. As the ionic force increases, the electrostatic charges of the modifier particles are screened, the particle-particle electrostatic repulsions are weaker and, consequently, the equilibrium density gradient is steeper[17]. The effect of the ionic and non-ionic solutes on the equilibrium concentration distribution of the silica-PVP particles was studied in detail just recently[17] as well as the repeatability of the established equilibrium distributions. The main conclusions following from these previous investigations which are relevant with respect to this study are:

-The NaCl ions influence the electrostatic repulsions and/or the effective hydrodynamic volume of the silica-PVP up to the concentration of 50 mM/l. Further increase of the NaCl concentration has no effect. As a result, the concentration of the NaCl can be used as a factor moderating the steepness of the equilibrium density gradient without changing the strenght of the centrifugal field forces.

-The investigated non-ionic solute (saccharose) had no effect on the equilibrium concentration distribution of the modifier particles even at the concentration as high as 390 mM/l. The only effect is the change of

the average density of the suspending liquid which must be taken into account. This is a very important finding because the PANI-PVA and PMTD-PVA particles could contain an excess of the non-ionic free PVA chains and aggregates[21]. As the volume fraction of the PANI-PVA or PMTD-PVA particles in focusing experiments is very low, it is evident that the concentration of the casual PVA chains and aggregates cannot have any detectable effect.

-The repeatability of the equilibrium density gradients as well as of the kinetics of the transient state was found very good under condition that the silica-PVP suspensions were kept closed to avoid the absorption of the aerial CO_2 which modifies the pH of the suspensions and, consequently, the ζ-potential of the modifier particles.

The first centrifugation experiments were thus aimed to determine the equilibrium distribution of the modifier silica-PVP particles and the time necessary to attain this equilibrium. Three different density marker beads added to the modifier suspension were used as the markers of the evolution of the density gradient until their steady-state equilibrium positions according to the technique proposed previously[18]. The results are demonstrated in Fig.5. The Fig.5a shows the evolution of the density gradient in the suspension without the addition of the NaCl while the Fig.5b shows the result obtained in a suspension of the same volume fraction $\phi = 0.0594$ but containing 50 mM/l NaCl. The density gradient formed in suspension with NaCl is steeper and the equilibrium is attained faster. The Fig.5c, concerning another centrifugation experiment carried out without the NaCl, shows very good repeatability of the evolution and of the steady-state density gradient. In this case, seven different densities marker beads were used. The Fig.5c demonstrates also the technique of the measurement of their equilibrium positions by computer processing of the scanned macrophotograph.

The $(U_m/D_m)_{eff}$ values were calculated from the eqns.(16) or (20) by using the non-linear regression to fit the experimental data: the equilibrium positions and densities of the density marker beads. Thus the $(U_m/D_m)_{eff}=0.4178$ cm^{-1} and $(U_m/D_m)_{eff}=2.433$ cm^{-1} values were obtained for the suspension without the NaCl and containing 50 mM/l NaCl, respectively.

Focusing Experiments

Based on our previous experience[17,18], the centrifugation focusing experiments were carried out under carefully chosen conditions, the centrifugal acceleration $g=1.962\text{x}10^3$ cm sec^{-2} (200 G), the average volume fraction of the silica-PVP suspension $\phi_{m,ave}=0.0594$, the height of the column of liquid in TLIF cell $h=20$ mm, the concentrations of the NaCl in density gradient forming liquids $c_{\mathrm{NaCl}}=0$ and 50 mM/l. The effect of the size ratio σ_p of the modifier to the fo-

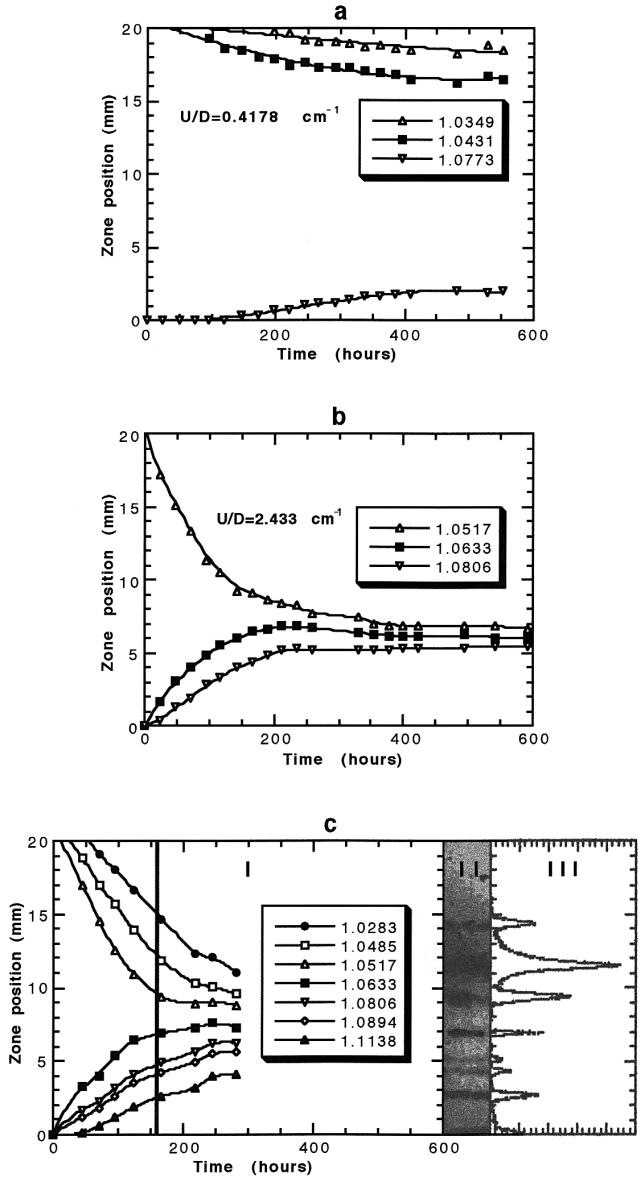

Figure 5. Evolution of the positions of the density marker beads (DMB) as a function of the centrifugation time. (**a**) Density gradient forming silica-PVP suspension without NaCl. (**b**) Density gradient forming silica-PVP suspension containing 50 mM/l NaCl. (**c**) The same experiment as in (**a**) but with seven DMB (**I**) and showing the picture (**II**) taken at 167 hours (see (**I**)) and the concentration distribution of all focused zones obtained by the image processing (**III**). The densities (g/ml) of the DMB are given for each experiment.

cused particles and the effect of the steepness of the density gradient on the width of the focused zone at equilibrium were studied with the use of four PANI-PVA samples of the average particle sizes of 231, 239, 443, and 451 nm and in two silica-PVP suspensions of the identical initial volume fraction $\phi = 0.0594$ but containing NaCl at two different concentrations of 0 and 50 mM/l. The results are shown in Figs.6 and 7 where the evolution of the focused zones is demonstrated at different stages of the centrifugation. The intermediate conclusions following from the qualitative evaluation of the results in Figs.6 and 7 are:

-As concerns the focusing in density gradient forming liquid without the NaCl, (Fig.6), the width of the zones decreases progressively during the centrifugation to become stable in equilibrium which is reached at the time determined as mentioned above.
-The PANI-PVA particles of smaller average size of 231 nm ($\sigma_p = 10$) exhibit much broader steady-state zone (Fig.6a) compared with larger particles (Fig.6b) of the average size of 443 nm ($\sigma_p = 19$). A small difference in relative polydispersities of these samples cannot explain the observed differences in the zone widths. In other words, this finding confirms the theoretical predictions resulting from the dynamic transport model.
-The evolution of the focused zones in density gradient forming liquid containing 50 mM/l NaCl shown in Fig.7 results in narrower zone in the case of smaller average particle size (Fig.7a) of 239 nm ($\sigma_p = 10$) of PANI-PVA as well as of larger particles (Fig.7b) of the average size of 451 nm ($\sigma_p = 20$) compared with the corresponding experiments without the NaCl in Fig.6. This also confirms the prediction concerning the effect of the steepness of the density gradient.
-Although the difference (Fig.7) in the widths of the focused zones of smaller (239 nm) and larger (451 nm) particle size samples is not so big as in the case without the addition of NaCl, still the result confirms the theory. Moreover, the observed difference is partly reduced by the fact that the relative polydispersity of smaller size sample was significantly lower than that of larger size one.

We observed the formation of the secondary zones in focusing experiment with density gradient forming liquids containing the NaCl and in a lesser extent in experiments without the NaCl. These secondary zones can clearly be seen especially in Fig.7. They appear and their positions go up during the centrifugation and remain stabilized when the equilibrium is attained. These secondary zones are uncolored and look like a liquid of different refractive index compared to the bulk liquid. We have taken few microlitres of the samples from the TLIF cell at different positions when the focusing experiments were finished and measured the PSD and average particle size of the micro-samples. The results are shown in Fig.8, to-

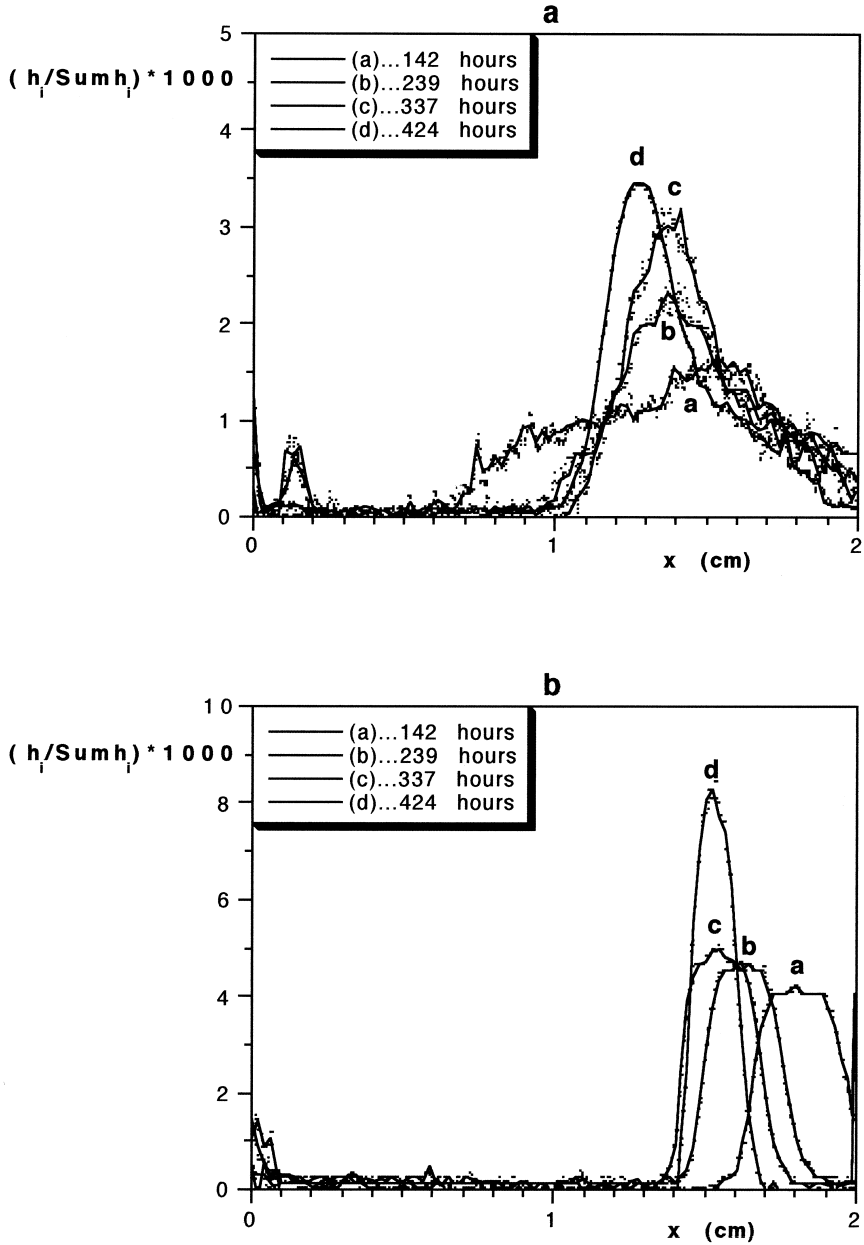

Figure 6. Evolution of the focused zones as a function of time of the PANI-PVA in density gradient forming silica-PVP suspension without the NaCl. Average particle diameter of the PANI-PVA: (**a**) 231 nm; (**b**) 443 nm.

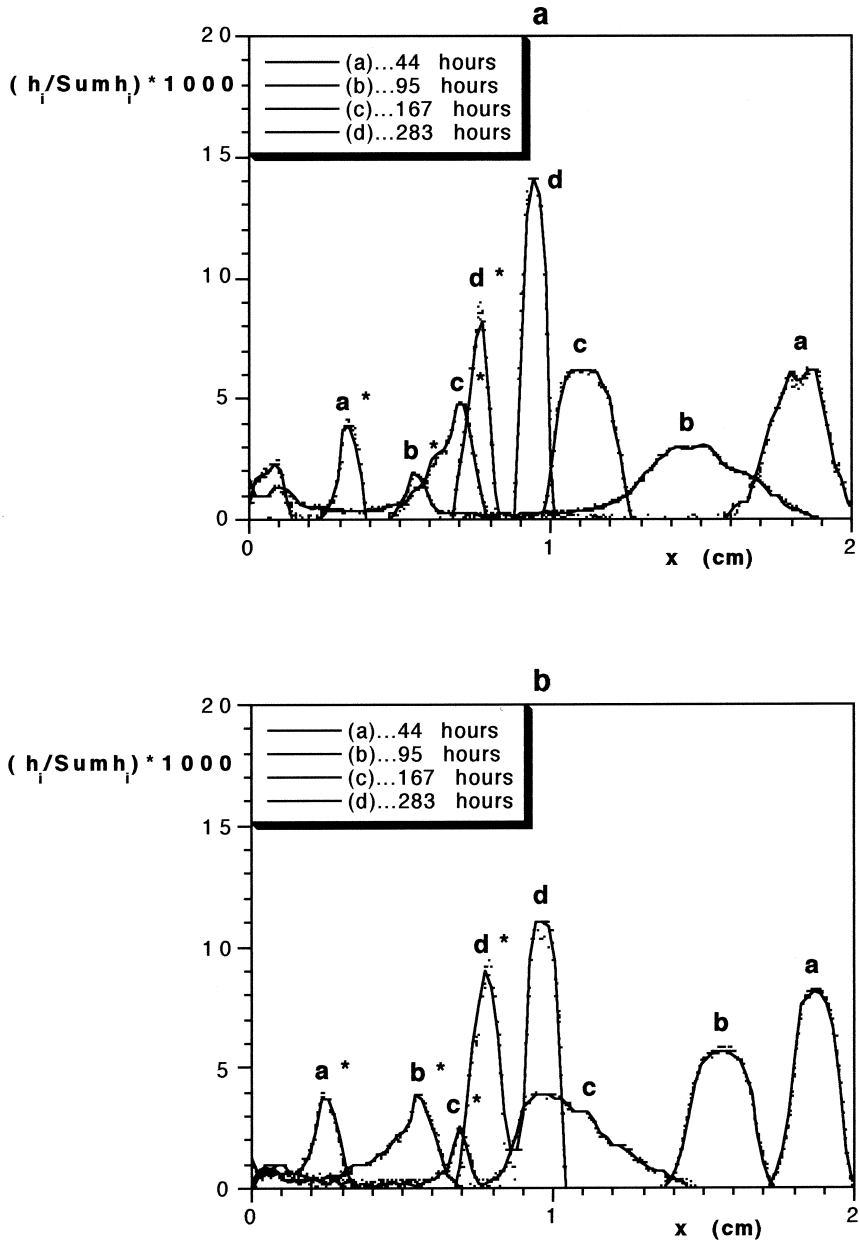

Figure 7. Evolution of the focused zones as a function of time of the PANI-PVA in density gradient forming silica-PVP suspension containing 50 mM/l NaCl. Average particle diameter of the PANI-PVA: (**a**) 239 nm; (**b**) 451 nm. *Secondary zones (see the text).

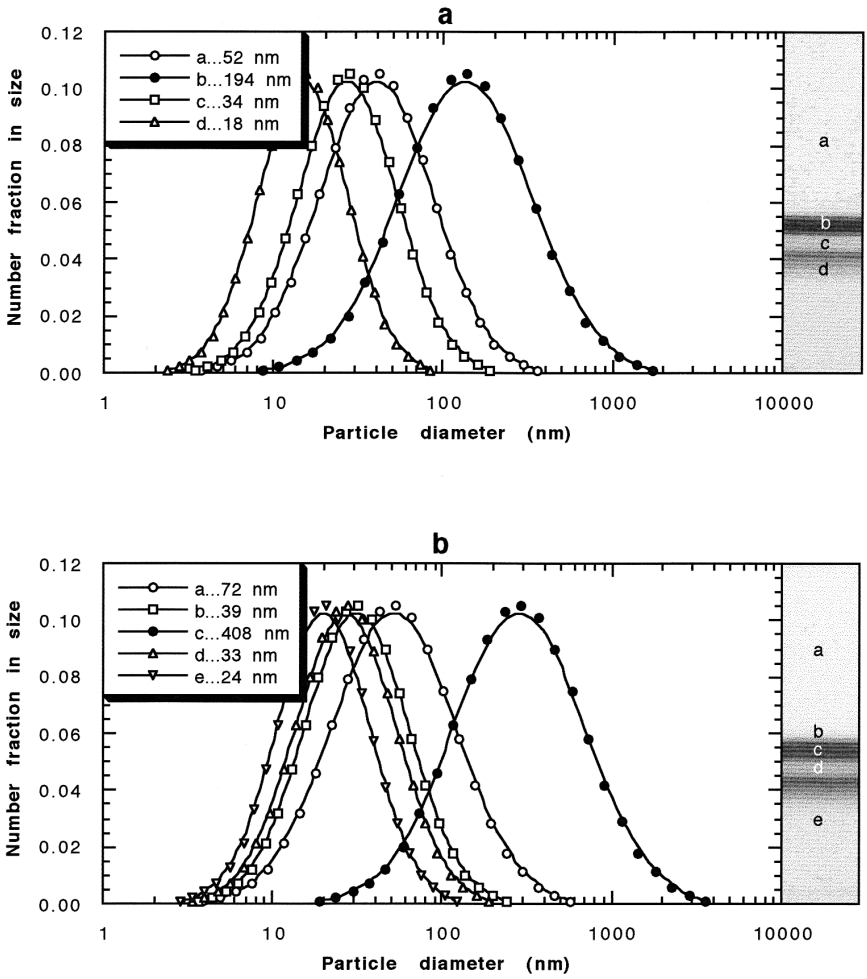

Figure 8. Particle size distributions measured by the quasi-elastic light scattering of the microsamples taken from the focused zones, secondary zones, zones neighborhood and bulk density gradient liquid. Focusing experiment with PANI-PVA samples of the average diameter: (**a**) 239 nm; (**b**) 451 nm.

gether with the macrophotographs of the TLIF cell with the focused zones and secondary zones under equilibrium conditions. Although the secondary zones were uncolored, the intensity of the black on the pictures is almost comparable with that of the focused zones. This is due to an intesive light scattering caused by these secondary zones.

The QELS measurements in Fig.8 show that, with the exception of the microsamples taken directly from the focused zones, the average particle size of other microsamples taken at different levels varies only slightly with the sampling position and corresponds approximately to the average particle size of silica-PVP. The average particle sizes of the microsamples taken from the focused zones are close to the average particle sizes of the concerned PANI-PVA samples (239 nm and 451 nm). The secondary zones could be some kind of the interfacial bands between differently organized stuctures of the type of liquid crystals or the transition regions between organized and non-organized liquid. However, this problem remains unresolved nowadays.

The average volume fractions of the focused particles were $\phi = 1.65 \text{x} 10^{-5}$ in all cases shown in Figs.6 and 7. The maximal volume fraction in the focused zone is roughly 10 to 20 times higher. Consequently, the minimal average distance between the focused particles corresponding to the maximal attained volume fraction is of the order of 17 to 10 particle diameters, calculated from:

$$n = \sqrt[3]{\frac{\phi_{max}}{\phi}} \tag{41}$$

where n is a multiple of the average particle size and $\phi_{max} = 0.78$ is the theoretically attainable maximal volume fraction for compact packing of uniform spheres in an unlimited space. On the other hand, the average distance of the modifier particles calculated from the average initial volume fraction is roughly 2.4 particle diameters. As these particles are at least 10 times smaller than the focused particles, it is reasonable to estimate that some 40 modifier particles, in average, can be interposed in a chaotic array within the mean space between two neighboring focused particles. As a result, the probability of the extensive interactions between the focused particles is low.

Regardless the above estimation, we have checked the effect of the volume fraction of the focused particles by decreasing further the average volume fraction by a factor 6. Such a dilution is about on the low limit of the accurate evaluation of the concentration distribution of the focused particles with respect to the intensity of the coloration and the subsequent image processing. The results of the focusing experiments in the density gradients media without and with the addition of the 50 mM/l of NaCl are shown in Fig.9. The widths of the focused zones of PANI-PVA sample of the average particle size of 451 nm are comparable, within the limits of experimental errors, with those obtained in experiments shown in Figs.6b and 7b with the only minor differences in the positions and the widths of the focused zones in Figs.6b and 9a which are due to minor differences in the densities and polydispersities between the PANI-PVA samples of 443 nm and 451 nm in diameter, respectively.

The last series of the centrifugation experiments was aimed to test the focusing with chemically different focused particles. The results with the use of

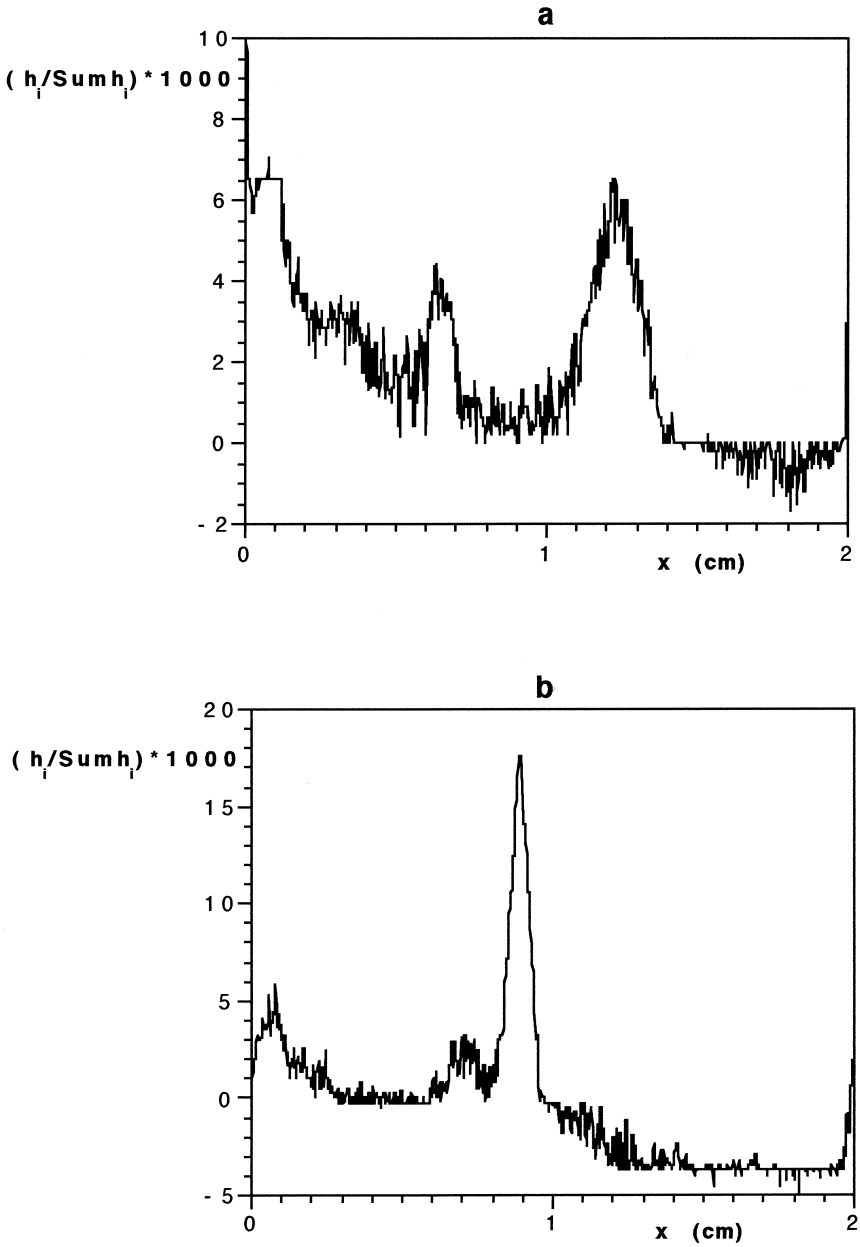

Figure 9. The equilibrium focused zones of the PANI-PVA sample of the average particle size of 451 nm in the density gradient forming liquids without the NaCl (**a**) and containing the NaCl at the concentration of 50 mM/l (**b**). The initial volume fraction of the PANI-PVA is 6x lower than in the experiment shown in Figs.6 and 7.

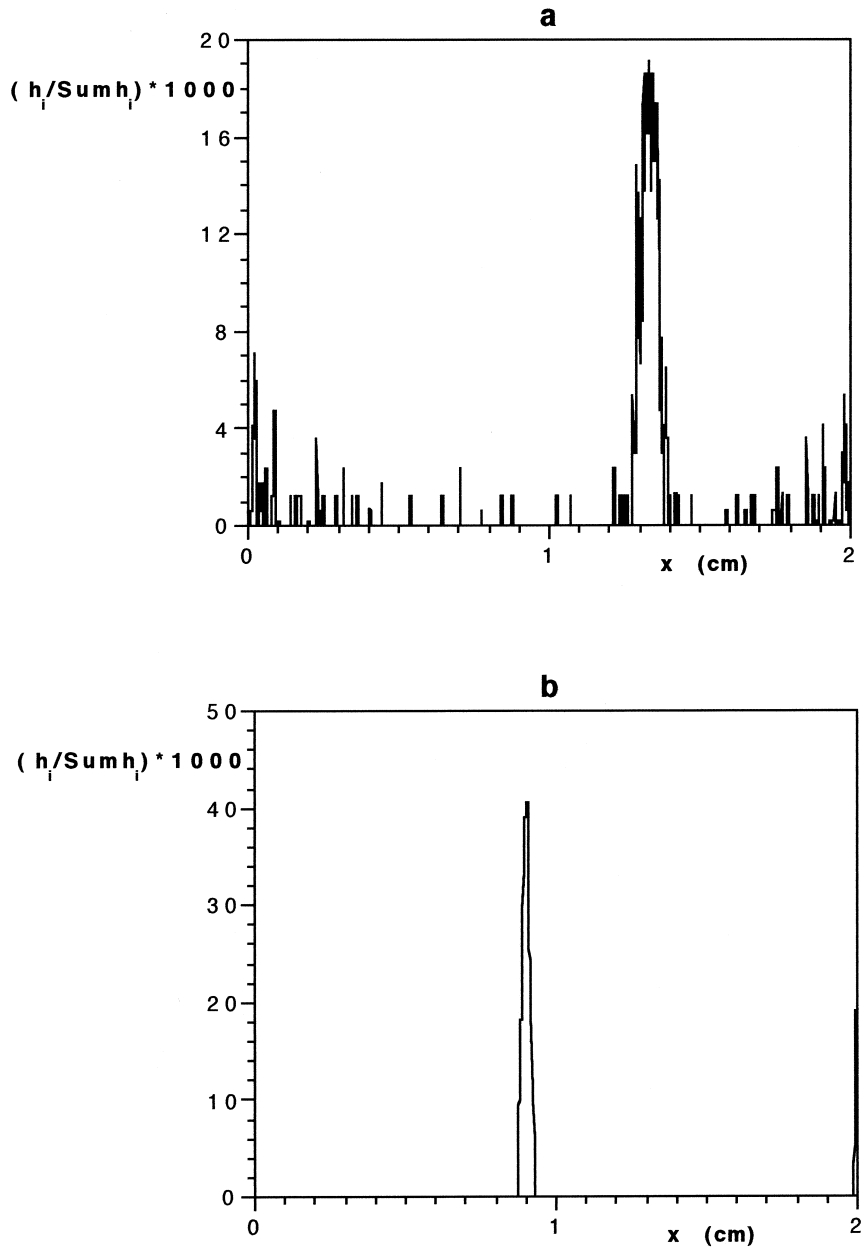

Figure 10. The equilibrium focused zones of the PMTD-PVA sample of the average particle size of 468 nm in the density gradient forming liquids without the NaCl (**a**) and containing the NaCl at the concentration of 50 mM/l (**b**).

the PMTD-PVA sample and a commercially available colored polystyrene microspheres of the average particle sizes of 468 nm and 655 nm, respectively, are demonstrated in Figs.10 and 11. Once again, the experiments were performed in density gradient media containing or not the NaCl. The focused zones in all cases are very narrow, in agreement with the theoretical considerations due to larger sizes of both tested samples. The narrowing of the zone focused in steeper density gradient in Fig.10 is evident but it is less pronounced in Fig.11 probably due to the fact that both zones (in presence and in absence of the NaCl) are already very narrow.

Comparison of Theoretical Models with Experiments

The centrifugal focusing experiments should allow to verify the conclusions of the developed models thus checking the correctness of our theoretical approach. This has been done by comparison of the theoretically calculated concentration distributions of the focused zones with the experimental ones by applying the eqn.(22). The results are shown in Figs.12 and 13 for which the experiments already demonstrated in Fig.6a, curve (d) and in Fig.11a, respectively, were used.

The density of the focused species should not be a priori known for the calculations using the eqn.(22), however it is implicitly related to the position of the maximal concentration $x_{i,max}$ which must be fixed. Thus the first statistical moments of the experimental concentration distributions were calculated and used as the $x_{i,max}$ values in corresponding calculations. The theoretical curves were calculated for hypothetically uniform size focused particles of the same diameter as the average particle diameter of the actually focused samples (curve (u) in Fig.12) and for the polydisperse samples (curve (p) in Fig.12) by taking into account the real PSD measured by the QELS of the corresponding samples.

The result in Fig.12 shows that the polydispersity of the concerned PANI-PVA sample does not play an important role, both theoretical curves are close each to other. On the other hand, the experimental concentration distribution (curve (e) in Fig.12) is even broader than the theoretical one calculated for polydisperse sample. The focused zone exhibits a tailing on the side closer to meniscus which does not seem to be caused by the PSD of the PANI-PVA sample. Similar comparisons were made for other focusing experiments with PANI-PVA and PMTD-PVA particulate samples, represented in Figs.6, 7, 9, and 10, with qualitatively the same results.

The focused zone of the colored polystyrene sample shown in Fig.13a is narrower due to larger size of this sample, as explained above. Its width lies well between the curves represented in Figs.13b and 13c, calculated for uniform and polydisperse particle populations, respectively.

The important difference between the PANI-PVA and PMTD-PVA particles, on one side, and the colored polystyrene microspheres, on the other, is that

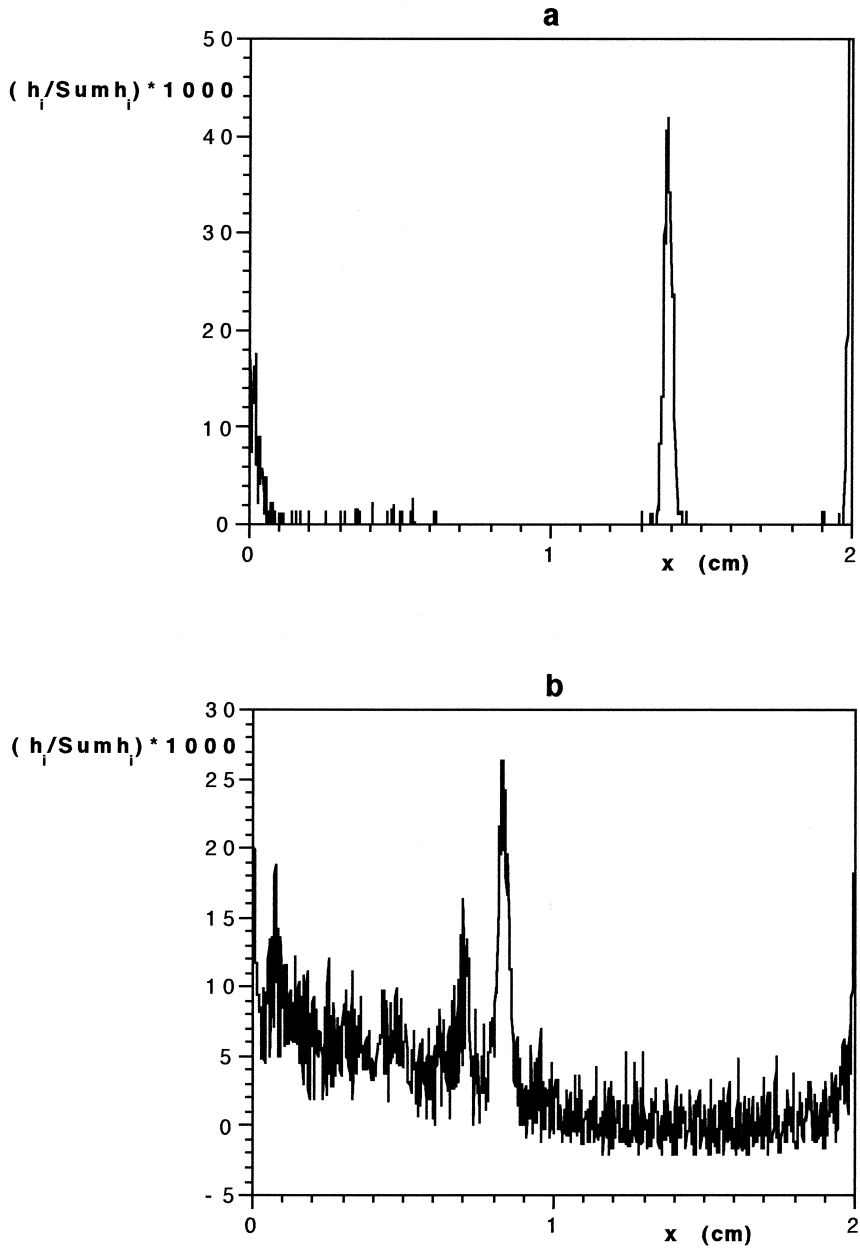

Figure 11. The equilibrium focused zones of the colored polystyrene sample of the average particle size of 655 nm in the density gradient forming liquids without the NaCl (**a**) and containing the NaCl at the concentration of 50 mM/l (**b**).

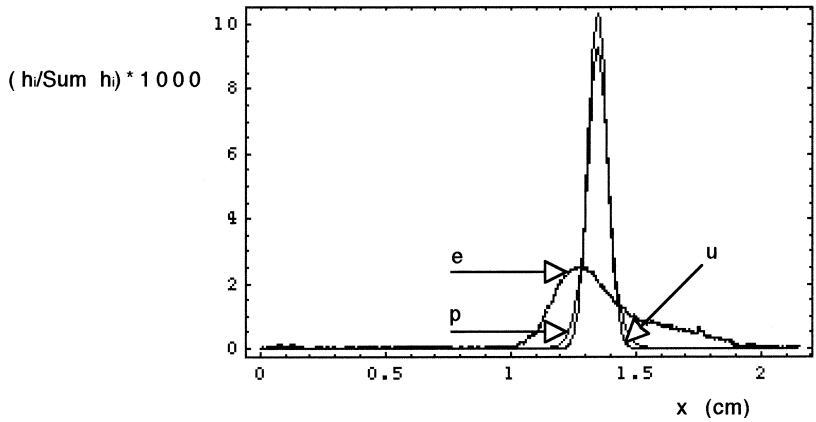

Figure 12. The comparison of the theoretically calculated equilibrium concentration distributions of the focused particles with the experimentally measured one (**e**). The calculated curves correspond to the uniform size focused particles (**u**) and to the polydisperse sample (**p**) of the same PSD as the real sample. The experimental curve is from the focusing shown in Fig.6a, curve d.

the first ones are covered by the "soft" PVA shell while the polystyrene particles can be considered as hard spheres. The flexibility of the PVA chains can allow a deformation of the soft shell due to the osmotic pressure gradient. This deformation decreases the chain entropy and creates an entropy gradient[25] leading to a displacement of the equilibrium position of the focused particles. The broadening and the observed tailing of the focused zone could be a natural consequence of such a behavior.

It must not be forgotten that the modifier particles used throughout the experiments in this work are the PVP covered silica, thus the "soft" spheres. As a result, the polymer-polymer interactions between the surface layers of the modifier and focused particles should also be taken into account. Althought the results of another experimental work[26] indicate that the NaCl causes a substantial shrinkage of the PVA chains and, consequently, the PANI-PVA and PMTD-PVA particles, undergoing the focusing under such conditions, approach to hard spheres, more extensive investigation is necessary to elucidate fully the effect of a salt on the effective behavior of the focused as well as of the modifier particles covered by a polymer.

Another driving force contributing to a displacement of the equilibrium position could be due to a reptation phenomenon. Whether or not such a phenomenon could arise under conditions of the focusing might be proved by comparing the kinetics of the transient states of the soft and hard particles of identical nature.

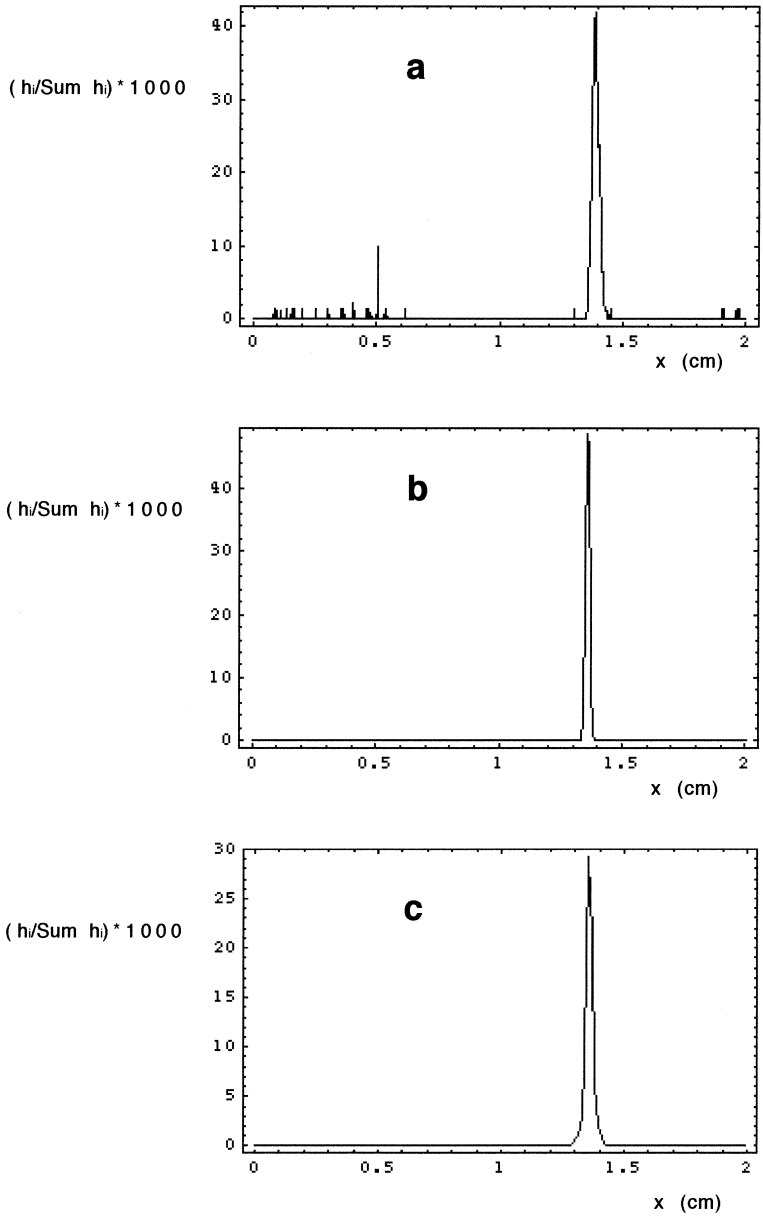

Figure 13. The comparison of the theoretically calculated equilibrium concentration distributions of the focused particles with the experimentally measured one (**a**). The calculated curves correspond to the uniform size focused particles (**b**) and to the polydisperse sample (**c**) of the same PSD as the real sample. The experimental curve is from the focusing shown in Fig.11a.

On the other hand, in a bidisperse colloidal suspension, such as any system exhibiting a focusing phenomenon, there is an attractive force between the larger focused particles. This force arises due to the entropic excluded-volume effect[27]. When the larger particles approach one another, the formerly occupied volume becomes available to the smaller particles which results in an increase of the entropy of the system. However, the supplementary experiments are needed in order to elucidate whether these effects can actually occur in the studied systems.

Focusing in Coupled Electric and Gravitational Fields

It has been postulated theoretically[28] and demonstrated experimentally[9,23] that the electric field instead of the centrifugal forces can be applied to form the density gradient in a suspension of charged colloidal silica particles, and the natural gravitation could be exploited to focus the uncharged or slightly charged larger particles. The first experiments[23] were carried out to demonstrate the focusing of the density marker beads whose diameter was 10000x larger than the diameter of the density gradient forming colloidal silica-PVP particles. The digital macrophotograph (I) of the six equilibrium focused zones of the density marker beads is shown in Fig.14a. In this case, it has been supposed that the dominating mechanism governing the behavior is the simple isopycnic focusing. This supposition was justified by the above mentioned very high size ratio of the focused to the density gradient forming modifier particles.

Later on[9], the first successful isoperichoric focusing generated by coupling the weak electric and gravitational fields and applied to the model bidisperse mixtures of the colloidal PANI-PVA and silica-PVP particles of low size ratio was described. A representative result of these focusing experiments is shown in Fig.14a. The macrophotographs of the TLIF cell in Fig.14a show the homogeneous concentration distribution of the PANI-PVA before the separation (II) and the equilibrium focused zone (III). The computer image processing resulted in a graphical representation of the focused zones of the DMB which is shown in Fig.14 b and the concentration distribution within the focused zone of the PANI-PVA particles shown in Fig.14c. The width of the focused zone was comparable with that calculated theoretically[9], however, a refinement is necessary from the experimental as well as the theoretical points of view. The main conclusion that can be drawn from these experiments is that the isoperichoric focusing principle exploiting the coupling of the electric and gravitational fields is reliable also for the effective separation of the particles whose size is not very different compared with the size of the density gradient forming colloidal particles.

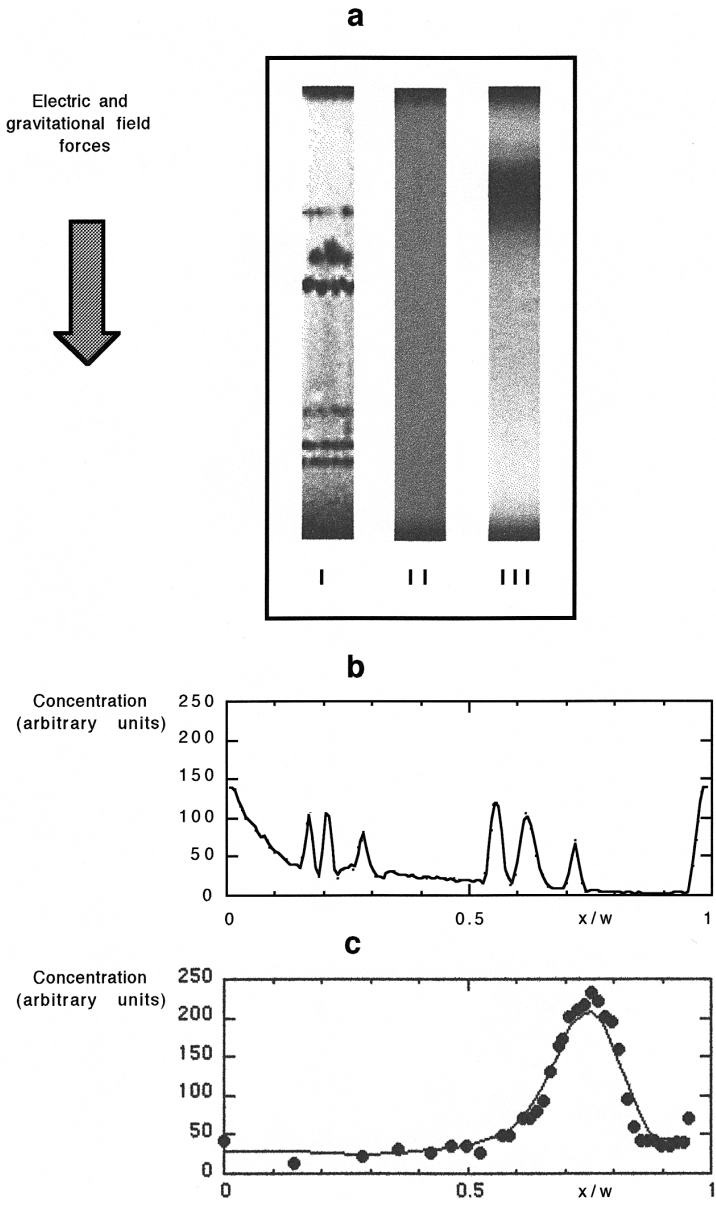

Figure 14. The isoperichoric focusing generated by the coupling of the electric and gravitational fields. The macrophotographs (a) of the focused large size density marker beads (**I**), of the initial homogeneous bidisperse mixture of the PANI-PVP with the silica-PVP (**II**) particles in the TLIF cell and of the equilibrium focused zone (**III**). The concentration distribution of the focused zones of the density marker beads (**b**) and of the PANI-PVP sample (**c**).

CONCLUSION

The new theoretical approach, based on the kinetic model, complements the formerly proposed dynamic transport model and both models hyphenated allow to understand more deeply the isoperichoric focusing effect and the accompanying transport phenomena and describe them on an accurate physical basis even when descending on a microscopic scale. It has been demonstrated throughout this paper that the theory and experiments fit quite well but we are aware that some refinements can still upgrade the present quantitative agreement.

The "isopycnic" focusing has for a longtime been used for the separation and characterization of the particles and large macromolecular and/or supramolecular structures. An enormous field of its practical applications concerns the particles of the biological origin such as the viruses, cells and subcellular fragments, etc. It is estimated that approximately 99 percent of all cell separations are performed in a centrifuge as a part of research experiment[23]. Certainly not negligible part of them is carried out by the "isopycnic" focusing even if other centrifugation methods and techniques are perfectly suited as well, but for other purposes[30–33]. As most of these biological species are the "soft" objects, one can imagine that the relationship between the experimental data from the "isopycnic" focusing separation and the concerned properties of the investigated matter is not so simple. The equilibrium positions of the focused zones will not coincide with the isopycnic layers whenever the particle-particle interactions (modifier-modifier, modifier-focused species, and focused species-focused species) will dominate the separation and, consequently, the simplistic mechanism based on a macroscopic model of the "isopycnic" focusing will no more be applicable.

The principal goal of this work was not "focused" on the analytical methodology aspects. As a result, this work does not provide an answer about a single property of the focused particles which could be drawn from the isoperichoric focusing experimental data. In this field, quite certainly many questions arose and extensive investigations are needed to transfer usefully some of the new physicochemical viewpoints discussed in this paper into a practical analytical application.

APPENDIX

There is a terminology problem concerning the common use of the term "dispersion" and the derived terms such as: monodisperse, bidisperse, polydisperse. . . species; as well as of the related quasi-synonyms such as: uniform, bicomponent, poly-component. . . etc. Moreover, the "dispersion" in *colloid science* is frequently used to denominate a dispersed matter such as a suspension, emulsion or even a consolidated porous structure. On the other hand, the term dispersion, etc., is used in *separation science* when dealing with the dispersive transport

processes driven, in general, by an entropic tendency to disperse (dilute) some species, concentrated somewhere within a limited space, into the whole available volume, by the molecular diffusion, Brownian motion, repulsive forces, etc. It is evident, that other sciences such as mathematics or computer science, etc., probably use the above terms in a completely different context. It would be a mission principally impossible and practically useless to try to redefine all these and related terms having for objective some kind of a unified terminology, independent of the scientific domain. As a result, we use throughout this paper the terms uniform, bidisperse and polydisperse matter when speaking about the size homogeneity or heterogeneity of the particulate matter regardless its chemical nature. When speaking about the transport phenomena and their consequences, we use systematically the term "dispersive processes". In order to avoid a confusion, we never use the term "dispersion" when speaking about a suspension.

REFERENCES

1. J. Montgolfier and E. Montgolfier, *Description des expériences aérostatiques de MM. de Montgolfier, et de celles auxquelles cette découverte a donné lieu*, Cuchet, Paris, 1784.
2. M. Meselson, F. W. Stahl, and J. Vinograd, *Proc. Natl. Acad. Sci. U. S. A.*, 1957, **43**, 581.
3. A. Kolin, *J. Chem. Phys.*, 1954, **22**, 1628.
4. H. Svensson, *Acta Chem. Scand.*, 1961, **15**, 325.
5. J. Janča, *Mikrochim. Acta* , 1994, **112**, 197.
6. J. Janča and M. Špáirková, *Collect. Czech. Chem. Commun.*, 1996, **61**, 819.
7. J. Janča, *J. Colloid Interface Sci.*, 1997, **189**, 51.
8. J. Janča, N. Caron, and N. Gospodinova, *J. Chem. Soc., Faraday Trans.*, 1998, **94**, 2961.
9. J. Janča, and N. Gospodinova, *Collect. Czech. Chem. Commun.*, 1998, **63**, 155.
10. A. Kolin, in *Electrofocusing and Isotachophoresis*, B. J. Radola and D. Graesslin, (Eds.), de Gruyter, Berlin, 1977.
11. S. E. Harding, J. C. Hordon, and A. J. Rowe, (Eds.), *Analytical Ultracentrifugation in Biochemistry and Polymer Science*, Royal Society of Chemistry, Cambridge, 1992.
12. G. M. Nazarian, *J. Phys. Chem.*, 1958, **62**, 1607.
13. A. Einstein, *Ann. Phys.* (Leipzig), 1906, **19**, 371.
14. J. Perrin, *C. R. Acad. Sci.*, 1908, **146**, 967.
15. G. K. Batchelor, *J. Fluid Mech.*, 1972, **52**, 245.
16. H. J. H. Clercx and P. P. J. M. Schram, *J. Chem. Phys.*, 1992, **96**, 3137.

17. J. Janča, N. Gospodinova, S. LeHen, and M. Špáirková, *J. Colloid Interface Sci.*, submitted.
18. J. Janča and M. Špáirková, *J. Colloid Interface Sci.*, 1996, **184**, 181.
19. J. Janča, in *Chromatographic Characterization of Polymers, Hyphenated and Multidimensional Techniques*, T. Provder, H. G. Barth, and M. W. Urban, (Eds.), ACS Advances in Chemistry Series 247, Washington, D. C., 1995.
20. N. Gospodinova and J. Janča, *Int. J. Polym. Anal. Charact.*, 1998, **4**, 323.
21. J. Janča, D. Moinard, E. Jančová, and N. Gospodinova, *Int. J. Polym. Anal. Charact.*, in press.
22. *Percoll: Methodology and Applications; Density Marker Beads for Calibration of Gradients of Percoll*, Pharmacia Fine Chemicals booklet.
23. J. Janča and R. Audebert, *Mikrochim. Acta* , 1993, **111**, 163.
24. J. Janča, *J. Appl. Polym. Sci., Appl. Polym. Symp.*, 1992, **51**, 91.
25. P. G. De Gennes, *J. Chem. Phys.*, 1974, **60**, 5030.
26. N. Gospodinova, E. Jančová, and J. Janča, unpublished results.
27. P. Pusey and W. van Megen, *Nature*, 1986, **320**, 340.
28. J. Janča and R. Audebert, *J. Appl. Polym. Sci., Appl. Polym. Symp.*, 1993, **52**, 63.
29. D. S. Kompala and P. Todd, Eds., *Cell Separation Science and Technology*, ACS Symposium Series 464, Washington, D.C., 1991.
30. K. L. Albright, L. S. Cram, and J. C. Martin, in D. S. Kompala and P. Todd, Eds., *Cell Separation Science and Technology*, ACS Symposium Series 464, Washington, D.C., 1991.
31. T. G. Pretlow and T. P. Pretlow, in D. S. Kompala and P. Todd, Eds., *Cell Separation Science and Technology*, ACS Symposium Series 464, Washington, D.C., 1991.
32. P. C. Keng, in D. S. Kompala and P. Todd, Eds., *Cell Separation Science and Technology*, ACS Symposium Series 464, Washington, D.C., 1991.
33. R. H. Davis, Ch.-Y. Lee, B. C. Batt, and D. S. Kompala, in D. S. Kompala and P. Todd, Eds., *Cell Separation Science and Technology*, ACS Symposium Series 464, Washington, D.C., 1991.